Lattice Boltzmann method for multiscale self-consistent field theory simulations of block copolymers

AIP | The Journal of Chemical Physics

Lattice Boltzmann method for multiscale self-consistent field theory simulations of block copolymers

Hsieh Chen, YongJoo Kim, and Alfredo Alexander-Katz

Citation: J. Chem. Phys. **138**, 104123 (2013); doi: 10.1063/1.4794922
View online: http://dx.doi.org/10.1063/1.4794922
View Table of Contents: http://jcp.aip.org/resource/1/JCPSA6/v138/i10
Published by the AIP Publishing LLC.

Lattice Boltzmann method for multiscale self-consistent field theory simulations of block copolymers

Hsieh Chen, YongJoo Kim, and Alfredo Alexander-Katz[a)]
Department of Materials Science and Engineering, Massachusetts Institute of Technology, Cambridge, Massachusetts 02139, USA

(Received 19 September 2012; accepted 26 February 2013; published online 14 March 2013)

A new Lattice Boltzmann (LB) approach is introduced to solve for the block copolymer propagator in polymer field theory. This method bridges two desired properties from different numerical techniques, namely: (i) it is robust and stable as the pseudo-spectral method and (ii) it is flexible and allows for grid refinement and arbitrary boundary conditions. While the LB method is not as accurate as the pseudo-spectral method, full self-consistent field theoretic simulations of block copolymers on graphoepitaxial templates yield essentially indistinguishable results from pseudo-spectral calculations. Furthermore, we were able to achieve speedups of $\sim 100\times$ compared to single CPU core implementations by utilizing graphics processing units. We expect this method to be very useful in multi-scale studies where small length scale details have to be resolved, such as in strongly segregating block copolymer blends or nanoparticle-polymer interfaces. © *2013 American Institute of Physics*. [http://dx.doi.org/10.1063/1.4794922]

I. INTRODUCTION

Block copolymer self-assembly has been shown to be a route for the production of exquisitely controlled patterns with sub-10 nm resolution that can be used in lithographic applications[1–6] and may one day find other important applications in functional materials or electronics.[7–9] The prediction of block copolymer morphologies by means of computer simulations is currently a topic of intense study due to the multiple potential applications. In this respect, Self-Consistent Field Theory (SCFT) has been shown to be invaluable in reproducing (and sometimes predicting) experiments with a high degree of fidelity.[10–15] Within the SCFT of block copolymers, one needs to evaluate the propagator of a single polymer in an external field which represents the probability of having a given monomer at a given position in space. This involves either directly sampling the configurations of the polymer using, for example, Monte Carlo methods,[16–19] or solving the associated Fokker-Planck equation for the evolution of the distribution function of the polymer that has the form of the diffusion equation in an inhomogeneous and time-dependent field.[20–23] Solving for this propagator constitutes the basis for obtaining the mean field free energy of the system and for evaluating other properties such as polymer densities. Here we explore a novel and complementary approach to this problem by utilizing a Lattice Boltzmann Method (LBM) for solving for the propagator.

In the last decade, SCFT has become the gold standard in the prediction of block copolymer morphology. One of the key advances was the solution of the diffusion equation using a pseudo-spectral (PS) method that allowed the use of large steps along the polymer chain while at the same time improving accuracy when constructing the propagator.[24–28] The pseudo-spectral method is also robust in that it is stable for all conditions. Previous methods, such as the semi-implicit Cranck-Nicholson approach, were marginally stable in 2D and only stable in 3D for time steps satisfying $\Delta t < \Delta x^2/8$.[29–31] However, one of the advantages of real space methods is that one can refine the meshes in situations where better local accuracy is necessary without sacrificing velocity of execution of the full domain. Such refinements are not possible in the traditional spectral methods because the box needs to be periodic. In order to alleviate this, Fredrickson and coworkers have developed very recently a new spectral scheme using Chebyshev polynomials[32] and studied the problem of wetting. In this work the authors used a constant mesh, but the fact that the boundary conditions are not periodic opens a route to perform multigrid simulations using this method.

A new alternative to finite discretization schemes is to use a lattice Boltzmann solver.[33,34] The solution to the underlying equations in this case emerges from a fluid lattice dynamics and has been used in many hard problems including turbulence.[35] This has several advantages: (i) it is intrinsically stable, (ii) the mesh can be locally refined,[36–41] (iii) arbitrary boundary conditions are straightforward to implement, and (iv) it is simple to parallelize and very fast codes already exist for multiple architectures.[42–45] The LB approach has been used extensively to solve the Navier-Stokes equations,[46–49] reaction diffusion problems,[50,51] finance problems,[52] etc. Thus, it constitutes a rather versatile approach to solving many different problems involving differential equations. Here we show that the LB approach is a viable alternative for SCFT simulations being at least comparable in speed (if not faster) than pseudo-spectral solvers. Our study is performed using Graphics Processing Units (GPUs) which are also a new and powerful alternative for massively parallel simulations.

This article is organized as follows: in Secs. II A and II B we provide a brief overview of polymer field

a)aalexand@mit.edu.

theory and how one can find a suitable solution to the fields, in particular concentrating on the case of diblock copolymers. In Sec. II C 1 we briefly explain the pseudo-spectral method and in Sec. II C 2 we introduce the LB method applied to the case of polymers. Our local refinement approach is introduced in Sec. II C 3. We then proceed in Sec. III A to characterize the accuracy of the LB method for different fields and in Sec. III B we show the SCFT simulations with local refinements. In Sec. III C we compute the morphologies of diblock copolymers on varying commensurate templates and in Sec. III D we provide benchmarks for the speed of the method. We finalize with concluding remarks.

II. THEORETICAL BACKGROUND AND METHODS

A. Field theory model

In this section we briefly present the model of an incompressible AB diblock copolymer melt.[53] Note that it is trivial to expand this model to triblock copolymers, polymer solutions, or polymer blends.[54] This model treats individual diblock copolymers in the continuous Gaussian chain description, includes a Flory-type contact interaction χ among dissimilar block segments (A and B), and constrains the total segment number density to a constant value ρ_0 at all points $\mathbf{r}$ in the system volume V (incompressibility condition). The block copolymers are assumed to be monodisperse with a total of N statistical segments; N_A segments of type A and $N_B = N - N_A$ segments of type B. Statistical segments are assumed to occupy equal volumes $v = 1/\rho_0$ and have equal segment lengths b. The average volume fraction of type A segments in the copolymer is denoted by $f = N_A/N$.

Through the use of Hubbard-Stratonovich-Edwards transforms, the segmental interactions in the above model can be decoupled with two auxiliary fields. Upon tracing out the chain coordinates, the nVT canonical partition function can be reexpressed as an interacting (classical) statistical field theory.[54,55] Scaling the lengths by the unperturbed radius of gyration $R_{go} = b\sqrt{N/6}$ and the curvilinear displacements s along the chain contour by N, the partition function is expressed as

$$Z \propto \int \mathcal{D}\Omega_+ \int \mathcal{D}\Omega_- e^{-H[\Omega_+,\Omega_-]}, \tag{1}$$

where the effective Hamiltonian is given by

$$H[\Omega_+, \Omega_-] = -C\{V \ln Q[\Omega_+, \Omega_-] + i\int d\mathbf{r}\Omega_+(\mathbf{r}) - \frac{1}{\chi N}\int d\mathbf{r}[\Omega_-(\mathbf{r})]^2\}. \tag{2}$$

The function $Q[\Omega_+, \Omega_-]$ corresponds to the partition function of a single polymer in the auxiliary fields $i\Omega_+$ (pure imaginary) and Ω_- (purely real), where $i \equiv \sqrt{-1}$. The two fields have different roles in the theory: Ω_+ can be interpreted as a fluctuating pressure that enforces incompressibility, while Ω_- is an exchange potential that defines the fluctuating composition profile in the AB copolymer melt. In particular, the latter field is conjugate to the local density difference between A and B defined as

$$\hat{\rho}_-(\mathbf{r}) = \hat{\rho}_A(\mathbf{r}) - \hat{\rho}_B(\mathbf{r}), \tag{3}$$

where $\hat{\rho}_A(\mathbf{r})$ and $\hat{\rho}_B(\mathbf{r})$ are the local density operators of the A and B type of monomers, respectively.

The single polymer partition function $Q[\Omega_+, \Omega_-]$ can be evaluated in the usual way,

$$Q[\Omega_+, \Omega_-] = \frac{1}{V}\int d\mathbf{r} q(\mathbf{r}, 1; [\Omega_+, \Omega_-]), \tag{4}$$

where the function $q(\mathbf{r}, s; [\Omega_+, \Omega_-])$ is a propagator that describes the probability of observing the s segment of the chain at position $\mathbf{r}$, given all possible placements of the first segment. This propagator satisfies the following modified diffusion equation

$$\frac{\partial}{\partial s} q(\mathbf{r}, s; [\Omega]) = \nabla^2 q(\mathbf{r}, s; [\Omega]) - \Omega(\mathbf{r}) q(\mathbf{r}, s; [\Omega]) \tag{5}$$

with the initial condition

$$q(\mathbf{r}, 0; [\Omega]) = 1 \tag{6}$$

and the field $\Omega(\mathbf{r})$ defined as

$$\Omega(\mathbf{r}) = \begin{cases} i\Omega_+(\mathbf{r}) - \Omega_-(\mathbf{r}), & \text{if } 0 < s \le f \\ i\Omega_+(\mathbf{r}) + \Omega_-(\mathbf{r}), & \text{if } f < s \le 1 \end{cases}. \tag{7}$$

Expressions for the reduced segment densities (volume fractions) in a block copolymer melt are well-known.[54] In particular, the reduced densities of A and B segments can be shown to be given by

$$\begin{aligned}\phi_A(\mathbf{r}; [\Omega_+, \Omega_-]) &= \frac{\rho_A(\mathbf{r}; [\Omega_+, \Omega_-])}{\rho_0}, \\ &= \frac{1}{Q}\int_0^f ds q^\dagger(\mathbf{r}, 1-s; [\Omega_+, \Omega_-]) \\ &\quad \times q(\mathbf{r}, s; [\Omega_+, \Omega_-])\end{aligned} \tag{8}$$

and

$$\begin{aligned}\phi_B(\mathbf{r}; [\Omega_+, \Omega_-]) &= \frac{\rho_B(\mathbf{r}; [\Omega_+, \Omega_-])}{\rho_0}, \\ &= \frac{1}{Q}\int_1^f ds q^\dagger(\mathbf{r}, 1-s; [\Omega_+, \Omega_-]) \\ &\quad \times q(\mathbf{r}, s; [\Omega_+, \Omega_-]),\end{aligned} \tag{9}$$

where f is as before the fraction of type A segment, $f = N_A/N$. The single diblock partition function Q and the propagator $q(\mathbf{r}, s; [\Omega_+, \Omega_-])$ are given by Eqs. (4) and (5), respectively. In the expressions we have also introduced a complementary propagator $q^\dagger(\mathbf{r}, s; [\Omega_+, \Omega_-])$, which is analogous to $q(\mathbf{r}, s; [\Omega_+, \Omega_-])$, but the propagation along the chain starts from the B end of the polymer. The $q^\dagger(\mathbf{r}, s; [\Omega_+, \Omega_-])$ propagator thus satisfies the following diffusion equation:

$$\frac{\partial}{\partial s} q^\dagger(\mathbf{r}, s; [\Omega]) = \nabla^2 q^\dagger(\mathbf{r}, s; [\Omega]) - \Omega(\mathbf{r}) q^\dagger(\mathbf{r}, s; [\Omega]), \tag{10}$$

with the initial condition

$$q^\dagger(\mathbf{r}, 0; [\Omega]) = 1 \tag{11}$$

and the field $\Omega(\mathbf{r})$ is now given by

$$\Omega(\mathbf{r}) = \begin{cases} i\Omega_+(\mathbf{r}) + \Omega_-(\mathbf{r}), & \text{if } 0 < s \le 1 - f \\ i\Omega_+(\mathbf{r}) - \Omega_-(\mathbf{r}), & \text{if } 1 - f < s \le 1 \end{cases}. \tag{12}$$

B. Numerical sampling algorithm

In this work we are interested in the so-called mean field solution (or SCFT solution) for the polymer field theory. Such an approach simply consists in minimizing the energy $H[\Omega_-, \Omega_+]$ and finding the fields Ω_-^* and Ω_+^* such that $\partial H/\partial\Omega_{+/-}|_{\Omega_{+/-}^*} = 0$.[53,54,56] In this work we use a simple explicit Euler forward scheme to do so. This approach has been shown to be useful in describing many properties in the self-assembly of block copolymers.[12–15] The "equations of motion" for the fields in such a scheme are given by

$$\Omega_-^j(t+\Delta t) = \Omega_-^j(t) - \Delta t\Gamma\frac{\partial H[\Omega_+^*, \Omega_-]}{\partial\Omega_-^j(t)} + \sqrt{\Delta t}\eta^j(t),$$
$$= \Omega_-^j(t) - \Delta t\Gamma C\{-\phi_-^j(t;[\Omega_+^*, \Omega_-])$$
$$+\frac{2}{\chi N}\Omega_-^j(t)\} + \sqrt{\Delta t}\eta^j(t), \quad (13)$$

where Ω_-^j and ϕ_-^j represent the value of the continuous field $\Omega_-(\mathbf{r})$ and continuous reduced density difference $\phi_-(\mathbf{r}) = \phi_A(\mathbf{r}) - \phi_B(\mathbf{r})$ at the cubic lattice site coordinates specified by the label $j = (j_x, j_y, j_z)$. The factor $\Gamma > 0$ is a constant relaxation rate. Notice that we add a term $\eta^j(t)$ which is a Gaussian real noise with first and second moments given by

$$\langle\eta^j(t)\rangle = 0 \quad (14)$$

and

$$\langle\eta^j(t)\eta^{j'}(t')\rangle = 2\Gamma'\delta_{j,j'}\delta_{t,t'}, \quad (15)$$

where Γ' is an arbitrary small constant used to avoid getting trapped in metastable points. This dynamics is utilized for all calculations and, as such, whatever effects appear from it will appear regardless of the method used to solve the diffusion equation which is the main contribution of this work.

For each update of the Ω_- field we relax the Ω_+ field as

$$\Omega_+^j(t+\Delta t) = \Omega_+^j(t) - \Delta t\frac{\partial H[\Omega_+, \Omega_-]}{\partial\Omega_+^j},$$
$$= \Omega_+^j(t) - \Delta t\Gamma iC\{\phi_+^j(t;[\Omega_+, \Omega_-]) - 1\}, \quad (16)$$

where as before Ω_+^j and ϕ_+^j represent the value of the continuous field $\Omega_+(\mathbf{r})$ and the continuous reduced total density $\phi_+(\mathbf{r}) = \phi_A(\mathbf{r}) + \phi_B(\mathbf{r})$ at the cubic lattice site coordinates specified by label j. We relax Ω_+ according to this scheme until the variance of the reduced total density ϕ_+^j averaged over the lattice, $\sigma^2 = \langle(\phi_+^j)^2\rangle - \langle\phi_+^j\rangle^2$, satisfies $\sigma^2 < 0.0001$, which implies that on average the local volume fraction is between 0.99 and 1.01 at each lattice point.

C. Solving the diffusion equation

1. Pseudo-spectral method

Solving the diffusion equation given by Eq. (5) is an integral part of the field-theoretic polymer simulations, since at each Langevin step its solution must be calculated for the particular realization of the field $\Omega(\mathbf{r})$. The pseudo-spectral method has been recognized as an accurate and efficient way,[24,25] which we will briefly describe below. The basic idea is that Eq. (5) can be formally solved as

$$q(\mathbf{r}, s+\Delta s) = \exp[\Delta s\nabla^2 - \Delta s\Omega(\mathbf{r})]q(\mathbf{r}, s), \quad (17)$$

where the value of the function at the contour location $s + \Delta s$ is constructed from knowledge of the function at the previous contour value $q(\mathbf{r}, s)$. In this way, the solution to Eq. (5) can be constructed by propagating the initial condition $q(\mathbf{r}, 0) = 1$ up to $s = 1$ through successive applications of the operator $\mathcal{L} = \exp[\Delta s\nabla^2 - \Delta s\Omega(\mathbf{r})]$. In principle this can be done, but the structure of $\mathcal{L}$ is complicated because the Laplacian operator ∇^2 and the field Ω do not commute. However, by use of the Baker-Hausdorff identity, the operator $\mathcal{L}$ can be conveniently approximated to yield an update scheme that is accurate to third order in Δs. This results in the following approximate update formula for the diffusion:

$$q(\mathbf{r}, s+\Delta s) \approx \exp\left[-\frac{\Delta s}{2}\Omega(\mathbf{r})\right]\exp[\Delta s\nabla^2]$$
$$\times\exp\left[-\frac{\Delta s}{2}\Omega(\mathbf{r})\right]q(\mathbf{r}, s). \quad (18)$$

The basic procedure now is as follows: First, the operator $e^{-(\Delta s/2)\Omega(\mathbf{r})}$ is applied at the lattice collocation points in real space. The resulting discretely sampled function is transformed to reciprocal space by a fast-Fourier transform (FFT) and the operator $e^{-\Delta s\mathbf{k}^2}$, corresponding to the discrete Fourier transform of $e^{\Delta s\nabla^2}$, is applied. An inverse FFT then restores the real space representation and the operator $e^{-(\Delta s/2)\Omega(\mathbf{r})}$ is finally applied at the lattice collocation points. The solution is then propagated forward by successive applications of the procedure just outlined.

2. Lattice Boltzmann method

The mathematical form of Eq. (5) is exactly the same as the so-called reaction-diffusion equation, which has been successfully and effectively solved by the LB method.[50,51] The LB method was originally developed as a mesoscopic particle-based numerical approach for solving fluid-dynamical equations.[35,57] However, more recently, the LB method has also been used as a general Laplace or Poisson equation solver.[58,59] Here we describe the LB method within the context of polymer field theory. The partition function propagators $q(\mathbf{r}, s)$ at each lattice site are accounted for by a one particle probability distribution $f_i(\mathbf{r}, s)$, where $\mathbf{r}$ is the lattice site, s is the curvilinear displacement, and the subscript i represents one of the finite spatial vectors $\mathbf{e}_i$ at each lattice node. The number and direction of the spatial vectors are chosen such that the resulting lattice is symmetric so as to easily reproduce the isotropy of the system.[59,60] The propagators at each site are calculated as

$$q(\mathbf{r}, s) = \sum_{i=0}^{n} f_i(\mathbf{r}, s), \quad (19)$$

where n is the total number of the spatial vectors.

During each contour step ds, distributions f_i stream along vectors $\mathbf{e}_i$ to the corresponding neighboring lattice sites and

collide locally. The most widely used variant of LB is the lattice Bhatnagar-Gross-Krook (BGK) model,[49,57] which approximates the collision step by a single time relaxation toward a local equilibrium distribution f_i^{eq}. The complete lattice BGK model (including the "reaction term" R[50,51]) is now written as

$$f_i(\mathbf{r}+\mathbf{e}_i dx, s+ds) - f_i(\mathbf{r}, s) = \frac{f_i^{eq}(\mathbf{r}, s) - f_i(\mathbf{r}, s)}{\tau} + w_i R, \tag{20}$$

where the reaction term equals to $R = \Omega(\mathbf{r})q(\mathbf{r}, s)$ and the equilibrium distributions satisfy[51]

$$f_i^{eq}(\mathbf{r}, s) = w_i q(\mathbf{r}, s). \tag{21}$$

It can be derived from the Chapman-Enskog analysis that the relaxation constant τ is related to the "diffusion coefficient" D of the relevant diffusion equation,[49,51,57] where D is effectively the prefactor in front of the Laplacian operator. For the normalized form in Eq. (5), the following relation holds:

$$D = 1 = c_s^2 ds(\tau - 0.5), \tag{22}$$

where $c_s = \frac{1}{\sqrt{3}}(dx/ds)$ is an effective "lattice speed" in the LB method.

The weights w_i depend in general on the dimension and the type of the lattice used. For two dimensional simulations, we use the nine direction model (D2Q9),[49,51,57] which gives the weights as

$$w_i = \begin{cases} 4/9, & \mathbf{e}_0 = (0,0) \\ 1/9, & \mathbf{e}_{1-4} = (\pm 1, 0), (0, \pm 1) \\ 1/36, & \mathbf{e}_{5-8} = (\pm 1, \pm 1) \end{cases}. \tag{23}$$

For three dimensional simulations, we use the nineteen direction model (D3Q19),[49,57] which gives the weights as

$$w_i = \begin{cases} 1/3, & \mathbf{e}_0 = (0,0,0) \\ 1/18, & \mathbf{e}_{1-6} = (\pm 1, 0, 0), (0, \pm 1, 0), (0, 0, \pm 1) \\ 1/36, & \mathbf{e}_{7-18} = (\pm 1, \pm 1, 0), (\pm 1, 0, \pm 1), (0, \pm 1, \pm 1) \end{cases}. \tag{24}$$

3. Local refinement

Under certain conditions, it would be more efficient to use locally refined patches of gridpoints, enabling a high resolution only where needed. The local refinement algorithm in the LB method has been developed by many researchers;[36–41] here we apply the procedure similar to the original work by Filippova and co-workers.[36] Grid refinement is performed by dividing the space step by a refinement factor m. The spacing and the contour steps on the fine grids are now given by

$$dx^f = \frac{dx^c}{m} \tag{25}$$

and

$$ds^f = \frac{ds^c}{m}, \tag{26}$$

where the superscripts "f" and "c" represent *fine* and *coarse* grids, respectively. In order to have a constant "diffusion coefficient" across the coarse and fine grids, the relaxation constant in the fine grids has to be redefined by[36]

$$\tau^f = \frac{1 + m(2\tau^c - 1)}{2}. \tag{27}$$

The numerical realization is the following. The whole computational domain is covered with the coarse grid and patches of fine grids are defined in certain regions. At a given step s_0, values of the distributions on the coarse grid which come from regions of finer patches are calculated in the nodes common to both grids according to

$$f_i^{post,c}(\mathbf{r}, s_0) = f_i^{post,f}(\mathbf{r}, s_0), \tag{28}$$

where $f_i^{post,c}$ and $f_i^{post,f}$ are the post collision distributions (but before streaming step) on the fine and coarse grids, respectively. At the step $s_1 = s_0 + ds^c$ (after one "stream-collision" step on the coarse grid), the new values of $f_i^{post,c}(\mathbf{r}, s_1)$ are known on the boundary of the fine patch. With interpolation $\tilde{f}_i^{post,c}$, one can calculate the values of $f_i^{post,f}(\mathbf{r}, s)$ according to

$$f_i^{post,f}(\mathbf{r}, s) = \tilde{f}_i^{post,c}(\mathbf{r}, s_1) \tag{29}$$

at steps $s = s_0, s_0 + ds^f, \ldots, s_0 + ds^f(m-1)$.

III. RESULTS AND DISCUSSION

A. Accuracy of the lattice Boltzmann method

Studies have shown that the pseudo-spectral method is highly accurate in solving diffusion equations.[24,25,54] Thus, it is ideal for us to compare the solutions from the lattice Boltzmann method to the solutions from the PS method and estimate the accuracy of the LB method. We construct the simplest testing scheme by solving a homopolymer melt with the initial condition $q(\mathbf{r}, s=0) = 1$ under a fixed field $\Omega(\mathbf{r})$ and comparing the propagators at the chain ends $q(\mathbf{r}, s=1)$ from different methods. In this testing scheme, we use square (2D) or cubic (3D) lattices with periodic boundary conditions of lengths $l_x = l_y = 3.2R_{go}$ or $l_x = l_y = l_z = 3.2R_{go}$. For a discretization $dx = 0.1$, the lattice sizes are $N_x = N_y = 32$ or $N_x = N_y = N_z = 32$. For $dx = 0.05$, the lattice sizes are $N_x = N_y = 64$ or $N_x = N_y = N_z = 64$. For the PS method, the chain discretization is set to $ds = 0.001$ ($N_s = 1000$) if not otherwise specified; for the LB method, we change ds continuously in order to find the minimum error (discussed in detail later).

We test three fields that we believe are most relevant to the simulations of block copolymers: (1) sine, (2) hyperbolic tangent, and (3) delta function fields. The first two fields have periodic forms that occur when the block copolymers pass order-disorder transitions.[61,62] Sine or hyperbolic tangent functions are used for weak or strong segregations,

$$\Omega_{\sin}(\mathbf{r}) = A \sin\left(M \frac{2\pi x}{N_x}\right) \tag{30}$$

and

$$\Omega_{\tanh}(\mathbf{r}) = \begin{cases} A \tanh\left(\frac{x - \frac{N_x}{4}}{\xi}\right), & \text{if } x < \frac{N_x}{2} \\ -A \tanh\left(\frac{x - \frac{3N_x}{4}}{\xi}\right), & \text{if } x >= \frac{N_x}{2} \end{cases}, \tag{31}$$

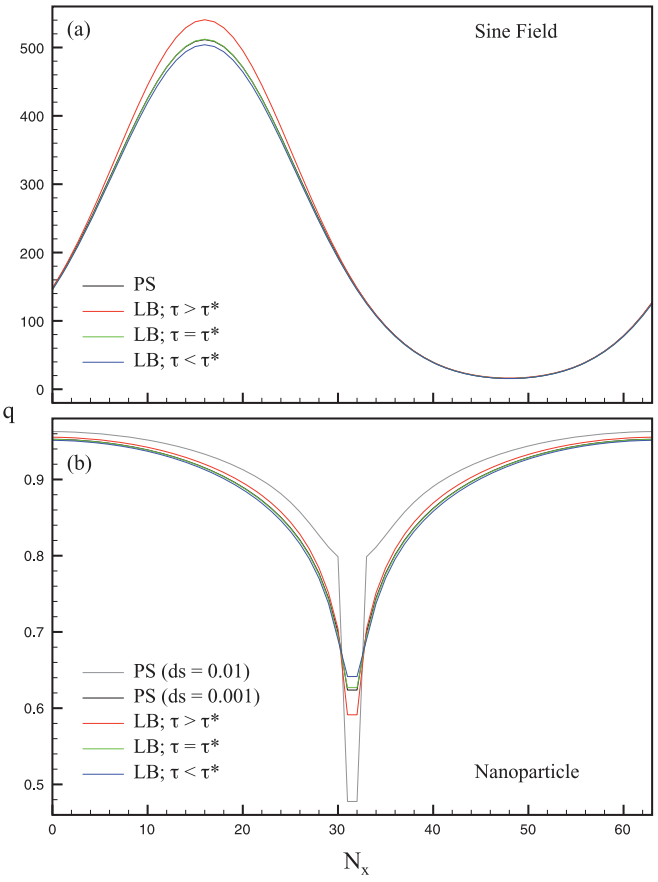

FIG. 1. Partition function propagators of a homopolymer at the chain ends $q(\mathbf{r}, s = 1)$ along the x direction under (a) sine and (b) nanoparticle fields solved from the pseudo-spectrum or LB methods. The space discretization is set to $dx = 0.05$. The LB relaxation constant is $\tau = 2.5$, $1.7(\sim \tau^*_{sin})$, and 1.1 for sine field and $\tau = 1.7$, $1.2(\sim \tau^*_{NP})$, and 0.8 for nanoparticle field.

where A is the field amplitude, M is the mode of the sine field, and ξ is a parameter that controls the sharpness of the hyperbolic tangent field at the transitions. The third field has a delta function form that is used for block copolymer systems with nanoparticles (NP)[63] or lithographical templates:[12,13,64]

$$\Omega_{NP}(\mathbf{r}) = \begin{cases} -100, & \text{if } \frac{N_x}{2} - 1 \le x \le \frac{N_x}{2} \\ & \frac{N_y}{2} - 1 \le y \le \frac{N_y}{2} \\ & \frac{N_z}{2} - 1 \le z \le \frac{N_z}{2} \text{ (for 3D)} \\ 0, & \text{otherwise} \end{cases}. \quad (32)$$

Figure 1 shows the representative calculated partition function propagators at the chain ends $q(\mathbf{r}, s = 1; [\Omega])$ along the x direction from both the PS and LB methods under the sine (Fig. 1(a)) or nanoparticle fields (Fig. 1(b)). For comparison purpose, we consider the solutions from the PS method (with $ds = 0.001$) as the exact solution. Interestingly, we find that the accuracy of the LB method is controlled by the relaxation constant

$$\tau = 3\frac{ds}{dx^2} + 0.5. \quad (33)$$

The observation that the accuracy of the LB method is controlled by τ has also been observed by other researchers when solving the reaction-diffusion equation.[51] Interestingly, for τ larger than a value that we here label τ^*, we find that the LB method overestimates q, while for τ smaller than τ^*, we find underestimate solutions (Fig. 1). This can be particularly seen in the case of a very localized external field, as would be a small nanoparticle. In principle, this is a very discouraging fact of solving the diffusion equation using a LB solver, but as will be shown below, this method becomes robust with respect to τ once the full SCFT is solved. Thus, it is not necessary to know *a priori* which is the best τ for solving the field theory. The reason for this behavior is a cancelation of errors when updating the fields, as will be discussed in detail in the end of this section. Additionally, it is important to notice that the PS scheme strongly loses its accuracy if we do not consider many steps along the chain. We find that for the nanoparticle field, the chain discretization $ds = 0.01$, which is a typical value in SCFT simulations, is not sufficient to obtain the accurate result. As shown in Fig. 1(b), the PS solution with $ds = 0.01$ has a very large discrepancy compared to the solution with $ds = 0.001$.

To systematically search τ^* for different fields, we define an error value[51]

$$\text{Error} = \sqrt{\frac{\Sigma_{\mathbf{r}}|q_{PS}(\mathbf{r}, s = 1) - q_{LB}(\mathbf{r}, s = 1)|^2}{\Sigma_{\mathbf{r}}|q_{PS}(\mathbf{r}, s = 1)|^2}}, \quad (34)$$

where q_{PS} and q_{LB} are the solutions from the PS and LB methods. Figure 2 shows the error values as a function of τ for different fields with different dimensions or dx. The amplitudes of the sine and hyperbolic tangent fields are chosen to be $A = 10$ here. It is clear that the critical τ^* where the minimum error occurs is not sensitive to dimensions or dx. For sin fields with mode = 1 and tanh fields, τ^* is around 1.7–2.2. However, for sin fields with mode > 1 and nanoparticle fields, τ^* decreases to 1.1–1.3. Although τ^* does not change with dx, the absolute errors decrease with decreasing dx. For $dx = 0.1$, the minimum errors range from 0.01 (for the tanh and sin fields) to 0.0005 (for the nanoparticle field). For $dx = 0.05$, the minimum errors are much smaller from 0.005 (for the tanh and sin fields) to 0.0001 (for the nanoparticle field). The minimum errors and τ^* also change with the field amplitudes A. Figure 3 shows the errors as a function of τ for sin (mode = 1; Fig. 3(a)) and tanh fields ($\xi = 1$; Fig. 3(b)) with field amplitudes $A = 4$ to 10. As shown, the minimum errors and τ^* both increase with increasing A. In addition, we observe that the optimal τ that results in minimum errors for $q(\mathbf{r}, s = 1)$ also results in minimum errors for $q(\mathbf{r}, 0 < s < 1)$. In Fig. 4 we show the error values for $q(\mathbf{r}, s)$ as a function of τ for $s = 0.4$, 0.6, 0.8, and 1.0. It is observed that for sine field with mode = 1 and amplitude = 10, $\tau^* \sim 1.7$ for all s.

After extensively testing the accuracy of the diffusion equation solver, we move on to use the LB method to perform the actual SCFT simulations. Figure 5(a) shows the mean-field results (with the noise field $\eta = 0$ in Eq. (13))[53] for the density distributions of a diblock copolymer system with $f = 0.5$ and $\chi N = 13$. Mild fields $\Omega_- = \pm 5$ to attract A or B blocks are applied at $x = 0$ or $x = \frac{N_x}{2}$ to induce the lamellar structure. To test the tolerance of the errors from the LB method for the lamellar structure formation, we perform simulations with $\tau = 2.5$, 1,7 ($\sim\tau^*$), and 1.1 with $dx = 0.05$.

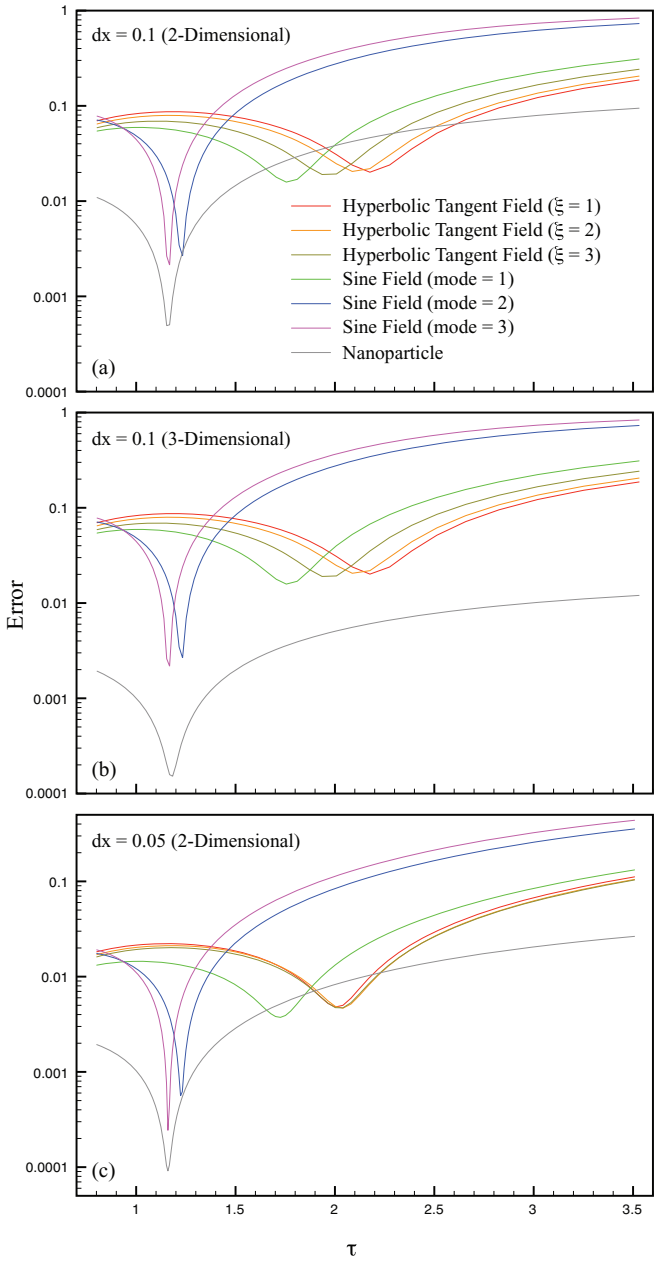

FIG. 2. Error values (see text for definition) as a function of the relaxation constant τ for different fields with (a) $dx = 0.1$ in 2D, (b) $dx = 0.1$ in 3D, and (c) $dx = 0.05$ in 2D.

Comparing this to the PS result, it is surprising that the final polymer density distributions from the LB method is undistinguishable from the PS results for all τ's even if we use nonoptimized τ's with higher errors. The errors in the densities and the equilibrium free energies are summarized in Fig. 5(b), where the errors in the densities are defined similar to Eq. (34) but with $q(\mathbf{r})$ substituted with $\phi(\mathbf{r})$, and the errors in the equilibrium free energies are defined as $|(H_{PS}^{eq} - H_{LB}^{eq})/H_{PS}^{eq}|$. We find that the errors in the free energies are about 2%–3%, which are comparable to the errors in $q(\mathbf{r}, s)$. However, it is very interesting that the errors in the densities are much smaller, which are only about 0.1%–0.5%. The more accurate densities may come from the normalization of $\int ds q^{\dagger} q$ with $Q \sim \int d\mathbf{r} q$, which cancels the errors in q when calculating

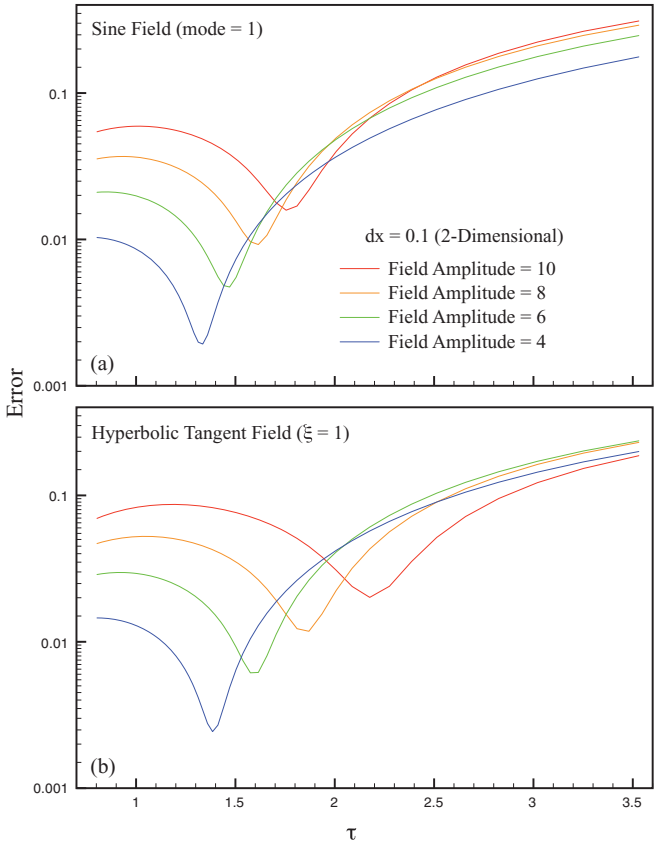

FIG. 3. Error values as a function of τ for (a) sin field (mode = 1) and (b) tanh field ($\xi = 1$) with different field amplitudes.

the densities using Eqs. (8) and (9). In conclusion, our results show that the LB method is robust since one does not need to know *a priori* the preferred τ. We believe the method is comparable with the PS method as an accurate solver for the polymer SCFT simulations, particularly if the self-consistent evolution of the fields only depends on the densities and the fields themselves. If higher accuracy in the calculation of the free energies is necessary, one can always interpolate the final configuration of the fields obtained using the LB method to a

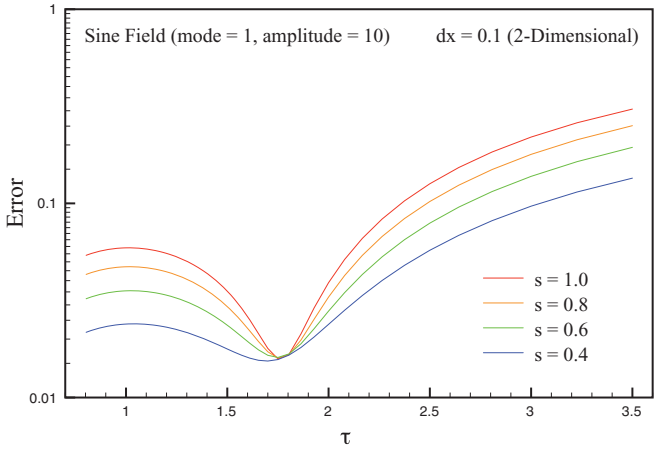

FIG. 4. Error values for $q(\mathbf{r}, s)$ as a function of τ for $s = 0.4$, 0.6, 0.8, and 1.0.

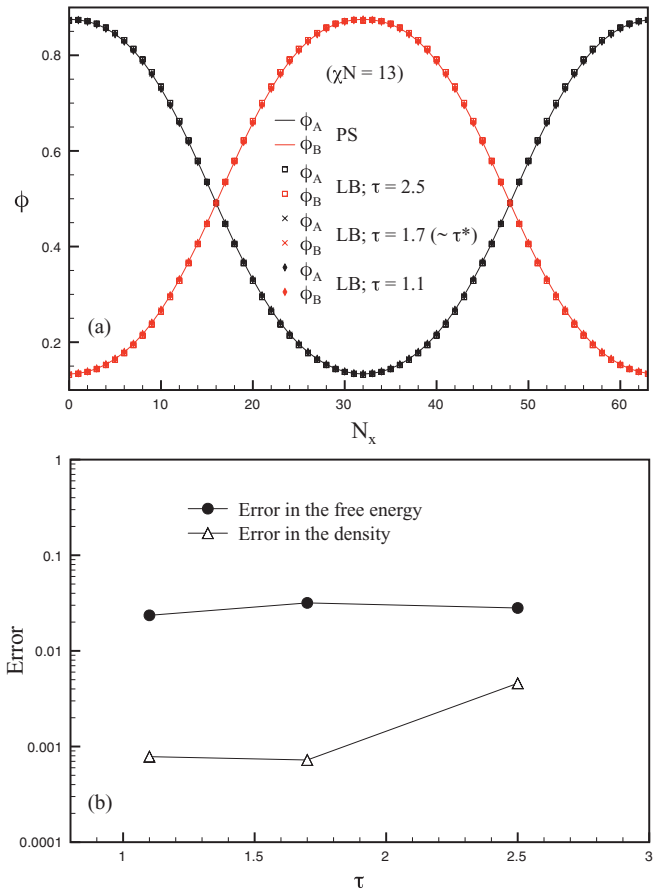

FIG. 5. (a) Density distributions of a diblock copolymer system with $f = 0.5$ and $\chi N = 13$ from SCFT simulations with the PS or LB methods. (b) Errors in the free energies and the densities comparing the LB result to the PS result.

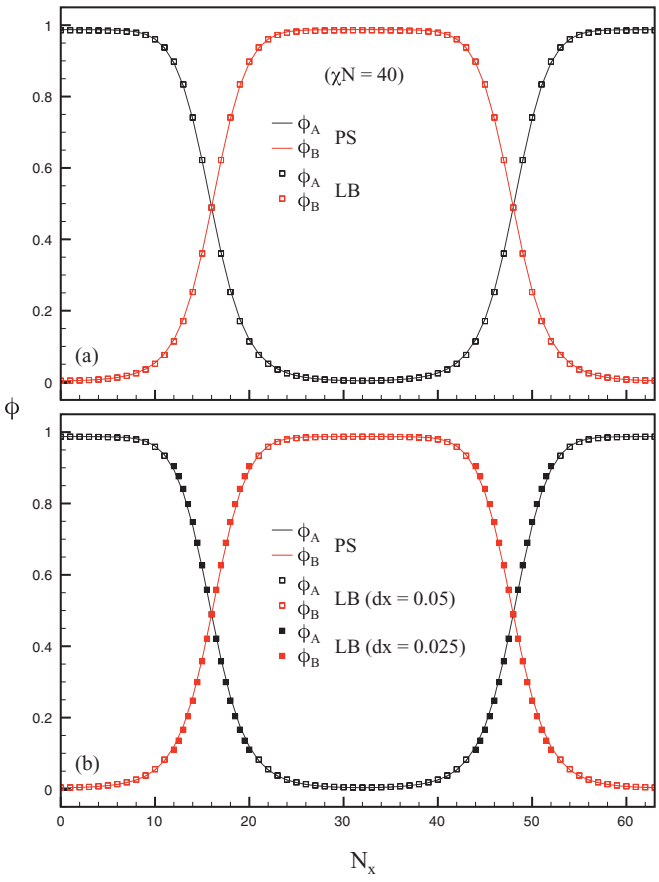

FIG. 6. Density distributions of a diblock copolymer system with $f = 0.5$ and $\chi N = 40$ (a) without or (b) with local refinements. The solid lines are the solutions from the pseudo-spectrum method and the symbols are the solutions from the lattice Boltzmann method.

finer grid and solve for the propagator only once. This might be very useful specially when dealing with multiple grids.

B. Multiscale SCFT simulations

Since the pseudo-spectral method evaluates the Laplacian in reciprocal space,[24,25] this method is only semi-local, and it has not yet been possible to apply local refinements. On the contrary, the lattice Boltzmann method is purely local in real space,[57] enabling us to apply fine patches locally. In SCFT simulations, the ability to apply finer discretization in specific regions is potentially more efficient since most of the computations can now be used to calculate the regions of interest. For block copolymer systems, when the interaction parameter χN increases, the interfaces between A and B blocks become sharper.[62] As a result, one would like to refine the interface regions in order to get higher resolution in this region. Figure 6 shows the density distributions of a diblock copolymer system with $f = 0.5$ and $\chi N = 40$ without (Fig. 6(a)) or with local refinements (Fig. 6(b)). Without refinements (Fig. 6(a)), the LB result again agrees perfectly well with the result from the PS method. However, sometimes the resolution of the uniform discretization $dx = 0.05$ may not be enough to resolve the interfacial regions. With local refinement, on the other hand, the interfacial regions can be much more finely resolved, as seen in Fig. 6(b). We find that the LB result with local refinement also agrees very well with the "exact" PS result even with simple first order (or linear) interpolation on the boundaries. Nevertheless, for more complex boundaries where this is not the case one could use higher order interpolation methods.[36–38] In the linear interpolation scheme we simply average out the values of the "velocity densities" and the mid points were the coarse and the fine grid meet. This operation scales as the size of the boundary (in 3D it scales as $N_{grid}^{2/3}$, where N_{grid} is the number of points inside the refined grid) and this interpolation is extremely fast. This is one of the advantages of the method we present here. For the case of the new spectral implementation using Chebyshev polynomials, which in principle could be used to perform multigrid simulations, one needs to recalculate the basis at each step along the field relaxation dynamics. Such an operation scales with the size of the refined box N_{grid}. As usual, both methods have their own appealing features: LB allows for a direct and fast multigrid approach, but lacks the accuracy (more on this below), while the new spectral methods have a higher accuracy but might be slower. We are still in the early stages of developing both methods and thus a precise comparison is not possible at this point.

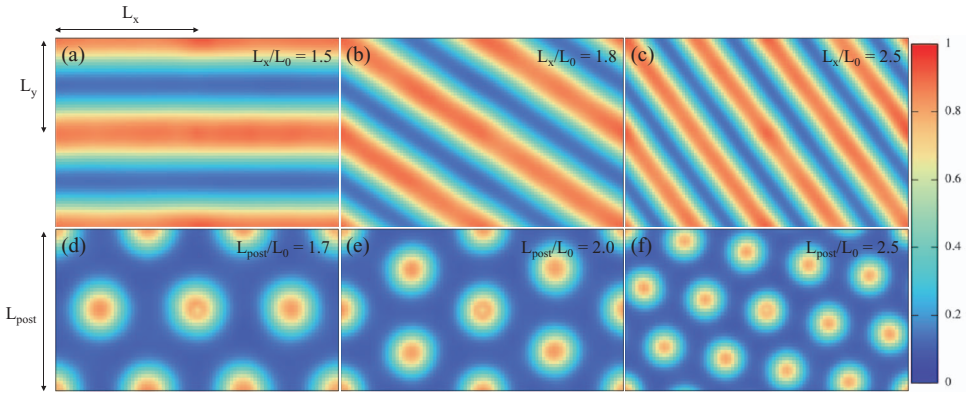

FIG. 7. 2D SCFT simulations of the self-assembly of block copolymers on commensurate templates using the LB method. The parameters of the copolymers are (a) to (c) $f = 0.5$ and $\chi N = 13$ and (d) to (f) $f = 0.25$ and $\chi N = 18$.

C. Self-assembly of block copolymers on varying commensurate templates

An active research area in engineering block copolymer morphologies is guiding block copolymers to self-assemble on lithographic templates to acquire special orientations or long range order.[12,13,65–69] Toward this end, SCFT simulations have been widely used to complement experiments in order to predict or verify the experimental results.[12,13,69] Here, we try to reproduce the experimental and theoretical findings from previous works using SCFT simulations with the lattice Boltzmann method. Figures 7(a)–7(c) show a diblock copolymer system with $f = 0.5$ and $\chi N = 13$ self-assembled on the predefined templates. The simulation boundary lengths (with periodic boundary conditions) are $l_x = 2L_x$ and $l_y = 2L_y$, where the ratio of L_x and L_y is fixed to $L_x/L_y = 1.5$. Four "posts" that attract A monomers are put on the positions $(x, y) = (0, 0)$, $(L_x, 0)$, $(0, L_y)$, and (L_x, L_y). When changing the ratio of L_x and the natural diblock copolymer length L_0 from $L_x/L_0 = 1.5$ to 2.5, we find that the lamellar orientations rotate in order to be commensurate with the post distances. These rotations agree perfectly well with prior studies.[12]

Figures 7(d)–7(f) show the diblock copolymer system with $f = 0.25$ and $\chi N = 18$. The simulation boundary lengths (with periodic boundary conditions) are $l_x = 1.75L_{post}$ and $l_y = L_{post}$. Two "posts" that attract A monomers are put on the positions $(x, y) = (0, 0)$ and $(0.875L_{post}, 0.5L_{post})$. Similar to the lamellar structures (Figs. 7(a)–7(c)), the cylindrical orientations rotate when changing the ratio L_{post}/L_0 (Figs. 7(d)–7(f)) in order to be commensurate with the distances between the posts. These rotations again agree particularly well with prior studies.[13] In summary, we show that SCFT simulations with the LB method yield indistinguishable results for the self-assembly of block copolymers on commensurate templates.

D. Benchmarking

For the last decade, general-purpose computation on graphics processing units (GPGPU) has become more and more popular in scientific computing. Very recently, Delaney and Fredrickson have used graphics processing units to implement polymer SCFT simulations with the pseudo-spectral method (SCFT-PS),[70] and acquired up to 60x acceleration compared to contemporary CPU cores. Because of a high degree of locality, the lattice Boltzmann method is a great candidate for GPU calculations.[58,71,72] We thus port our SCFT simulations with the LB method (SCFT-LB) to a GPU architecture. We compare the runtime of SCFT-LB or SCFT-PS running on a GPU (NVIDIA Tesla C2050) to the runtime of SCFT-PS on a desktop CPU (Intel Core 2 Duo 2.4GHz). Figure 8 shows the runtime per iteration ($ds = 0.01$) as a function of the total number of lattice points for different processing units and methods. For SCFT-PS on a GPU, the runtime per iteration increases from 0.02 to 0.5 s when increasing the number of lattice points from 4096 to 104 8576. On the other hand, for SCFT-PS on a CPU, the runtime per iteration increases from 0.02 to 20 s when changing the same number of lattice points. We would like to point out that, without extensive optimization, our runtime for SCFT-PS is very close to those obtained by Delaney and Fredrickson.[70] For SCFT-LB, it is more desirable to consider 2D and 3D separately since the number of "spatial directions" are different, where there are 19 directions in 3D but only 9 directions in 2D. On a GPU, the computation speed for 3D SCFT-LB is comparable with SCFT-PS for a number of lattice point higher than 10^5 and slightly faster for a number of lattice point smaller than 10^5.

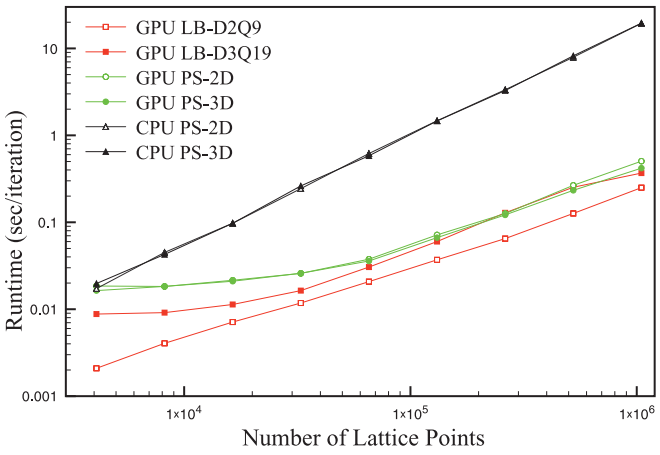

FIG. 8. Runtime per iteration as a function of the total number of lattice points for different processing units and methods.

For 2D SCFT-LB, the computation speed is about 2 × faster than SCFT-PS for a number of lattice point higher than 10^5 and is up to 10 × faster for a number of lattice point smaller than 10^4. In summary, we demonstrate that the LB method is very efficient to perform SCFT simulations on GPUs.

IV. CONCLUSIONS

In this work we have presented a novel approach employing lattice Boltzmann theory to solve for the propagator in SCFT. We have demonstrated that our hybrid LB-SCFT approach is capable of reproducing the results obtained with the pseudo-spectral method. Interestingly, the agreement between both when actually solving the full field solution exhibited errors much smaller than when considering single modes of the fields. An advantage of the LB method, however, is that one can consider local refinement of the mesh, while still retaining unconditional stability. While this is not as important for pure diblock copolymers, this improvement will certainly become important in blends that include homopolymers or in systems where disparate length scales appear. Furthermore, the LB method is very flexible and can be implemented under many different types of lattices and boundary conditions. For example one can also work in unstructured lattices[73–75] or apply complex boundary conditions either directly or through well developed immersed boundary methods.[76] Our implementation on a GPU reached ∼100 × improvement in the computation speed for 2D lattices and ∼60 × speedups for 3D lattices compared to a CPU implementation. However, as mentioned above, new methods using spectral algorithms with high precision are also emerging.[32] Such methods could be used in multigrid calculations and it is up to the researcher to choose a method depending on the problem requirements. Nevertheless, we believe the LB method nicely complements current SCFT methods and we have introduced it in the present work.

ACKNOWLEDGMENTS

H.C. and A.A.-K. acknowledge support by the National Science Foundation (NSF) under Award # DMR-1054671 (implementation of LB for SCFT); YJ.K. acknowledges support by the Center for Excitonics, an Energy Frontier Research Center funded by the U.S. Department of Energy (DOE), Office of Science, Basic Energy Sciences (BES), under Award # DE-SC0001088 (SCFT of block copolymers).

[1] T. Thurn-Albrecht, J. Schotter, G. A. Kastle, N. Emley, T. Shibauchi, L. Krusin-Elbaum, K. Guarini, C. T. Black, M. T. Tuominen, and T. P. Russell, Science **290**, 2126 (2000).
[2] S. O. Kim, H. H. Solak, M. P. Stoykovich, N. J. Ferrier, J. J. de Pablo, and P. F. Nealey, Nature (London) **424**, 411 (2003).
[3] J. Y. Cheng, C. A. Ross, H. I. Smith, and E. L. Thomas, Adv. Mater. **18**, 2505 (2006).
[4] J. Y. Cheng, A. M. Mayes, and C. A. Ross, Nature Mater. **3**, 823 (2004).
[5] J. Y. Cheng, C. A. Ross, E. L. Thomas, H. I. Smith, and G. J. Vancso, Appl. Phys. Lett. **81**, 3657 (2002).
[6] C. Tang, E. M. Lennon, G. H. Fredrickson, E. J. Kramer, and C. J. Hawker, Science **322**, 429 (2008).
[7] V. P. Chuang, W. Jung, C. A. Ross, J. Y. Cheng, O.-H. Park, and H.-C. Kim, J. Appl. Phys. **103**, 074307 (2008).
[8] K. Thorkelsson, A. J. Mastroianni, P. Ercius, and T. Xu, Nano Lett. **12**, 498 (2012).
[9] J. Kao, P. Bai, V. P. Chuang, Z. Jiang, P. Ercius, and T. Xu, Nano Lett. **12**, 2610 (2012).
[10] N. Koneripalli, F. S. Bates, and G. H. Fredrickson, Phys. Rev. Lett. **81**, 1861 (1998).
[11] Y. Wu, G. Cheng, K. Katsov, S. W. Sides, J. Wang, J. Tang, G. H. Fredrickson, M. Moskovits, and G. D. Stucky, Nature Mater. **3**, 816 (2004).
[12] J. K. W. Yang, Y. S. Jung, J.-B. Chang, R. A. Mickiewicz, A. Alexander-Katz, C. A. Ross, and K. K. Berggren, Nat. Nanotechnol. **5**, 256 (2010).
[13] R. A. Mickiewicz, J. K. W. Yang, A. F. Hannon, Y. S. Jung, A. Alexander-Katz, K. K. Berggren, and C. A. Ross, Macromolecules **43**, 8290 (2010).
[14] A. Tavakkoli K. G., K. W. Gotrik, A. F. Hannon, A. Alexander-Katz, C. A. Ross, and K. K. Berggren, Science **336**, 1294 (2012).
[15] A. Tavakkoli K. G., A. F. Hannon, K. W. Gotrik, A. Alexander-Katz, C. A. Ross, and K. K. Berggren, Adv. Mater. **24**, 4249 (2012).
[16] K. Ch. Daoulas, M. Muller, J. J. de Pablo, P. F. Nealey, and G. D. Smith, Soft Matter **2**, 573 (2006).
[17] F. A. Detcheverry, D. Q. Pike, P. F. Nealey, M. Meuller, and J. J. de Pablo, Phys. Rev. Lett. **102**, 197801 (2009).
[18] D. Q. Pike, F. A. Detcheverry, M. Meuller, and J. J. de Pablo, J. Chem. Phys. **131**, 084903 (2009).
[19] F. A. Detcheverry, D. Q. Pike, U. Nagpal, and J. J. de Pablo, Soft Matter **5**, 4858 (2009).
[20] J. G. E. M. Fraaije, J. Chem. Phys. **99**, 9202 (1993).
[21] J. G. E. M. Fraaije, B. A. C. van Vlimmeren, N. M. Maurits, M. Postma, O. A. Evers, C. Hoffmann, P. Altevogt, and G. Goldbeck-Wood, J. Chem. Phys. **106**, 4260 (1997).
[22] F. Drolet and G. H. Fredrickson, Phys. Rev. Lett. **83**, 4317 (1999).
[23] G. H. Fredrickson, V. Ganesan, and F. Drolet, Macromolecules **35**, 16 (2002).
[24] K. O. Rasmussen and G. Kalosakas, J. Polym. Sci., Part B: Polym. Phys. **40**, 1777 (2002).
[25] S. W. Sides and G. H. Fredrickson, Polymer **44**, 5859 (2003).
[26] T. L. Chantawansri, S. M. Hur, C. J. Garcia-Cervera, H. D. Ceniceros, and G. H. Fredrickson, J. Chem. Phys. **134**, 244905 (2011).
[27] H. D. Ceniceros and G. H. Fredrickson, SIAM Multiscale Model. Simul. **2**, 452 (2004).
[28] E. M. Lennon, G. O. Mohler, H. D. Ceniceros, C. J. Garcia-Cervera, and G. H. Fredrickson, SIAM Multiscale Model. Simul. **6**, 1347 (2008).
[29] V. Ganesan and G. H. Fredrickson, Europhys. Lett. **55**, 814 (2001).
[30] K. W. Morton and M. J. Baines, *Numerical Methods for Fluid Dynamics II* (Clarendon, 1986).
[31] A. Alexander-Katz, A. G. Moreira, and G. H. Fredrickson, J. Chem. Phys. **118**, 9030 (2003).
[32] S.-M. Hur, C. J. Garcia-Cervera, and G. H. Fredrickson, Macromolecules **45**, 2905 (2012).
[33] F. J. Higuera, S. Succi, and R. Benzi, Europhys. Lett. **9**, 345 (1989).
[34] F. J. Higuera and J. Jimenez, Europhys. Lett. **9**, 663 (1989).
[35] M. Briscolini, P. Santangelo, S. Succi, and R. Benzi, Phys. Rev. E **50**, R1745 (1994).
[36] O. Filippova and D. Hanel, J. Comput. Phys. **147**, 219 (1998).
[37] C.-L. Lin and Y. G. Lai, Phys. Rev. E **62**, 2219 (2000).
[38] A. Dupuis and B. Chopard, Phys. Rev. E **67**, 066707 (2003).
[39] D. Alemani, B. Chopard, J. Galceran, and J. Buffle, Phys. Chem. Chem. Phys. **8**, 4119 (2006).
[40] M. Stiebler, J. Tolke, and M. Krafczyk, Comput. Math. Appl. **55**, 1576 (2008).
[41] R. G. M. van der Sman and M. H. Ernst, J. Comput. Phys. **160**, 766 (2000).
[42] H. J. Limbach, A. Arnold, B. A. Mann, and C. Holm, Comput. Phys. Commun. **174**, 704 (2006).
[43] W. Li, X. M. Wei, and A. Kaufman, Visual Comput. **19**, 444 (2003).
[44] M. Bernaschi, S. Melchionna, S. Succi, M. Fyta, E. Kaxiras, and J. K. Sircar, Comput. Phys. Commun. **180**, 1495 (2009).
[45] M. Bernaschi, M. Fatica, S. Melchionna, S. Succi, and E. Kaxiras, Concurrency Comput.: Pract. Exper. **22**, 1 (2010).
[46] R. Benzi, S. Succi, and M. Vergassola, Phys. Rep. **222**, 145 (1992).
[47] S. Chen and G. D. Doolen, Annu. Rev. Fluid Mech. **30**, 329 (1998).
[48] S. Succi, E. Foti, and F. Higuera, Europhys. Lett. **10**, 433 (1989).
[49] Y. Qian, D. d'Humieres, and P. Lallemand, Europhys. Lett. **17**, 479 (1992).
[50] S. Ponce Dawson, S. Chen, and G. D. Doolen, J. Chem. Phys. **98**, 1514 (1993).
[51] S. G. Ayodele, F. Varnik, and D. Raabe, Phys. Rev. E **83**, 016702 (2011).
[52] J. Cerda, C. Montoliu, and R. J. Colom, Math. Comput. Modell. **57**, 1648 (2013).

[53]A. Alexander-Katz and G. H. Fredrickson, Macromolecules **40**, 4075 (2007).
[54]G. H. Fredrickson, *The Equilibrium Theory of Inhomogeneous Polymers* (Oxford University Press, England, 2006).
[55]M. W. Matsen and M. Schick, Phys. Rev. Lett. **72**, 2660 (1994).
[56]D. Duechs, V. Ganesan, and G. H. Fredrickson, Macromolecules **36**, 9237 (2003).
[57]S. Succi, *The Lattice-Boltzmann Equation: For Fluid Dynamics and Beyond* (Clarendon, Oxford, 2001).
[58]Y. Zhao, Visual Comput. **24**, 323 (2008).
[59]S. P. Thampi, S. Ansumali, R. Adhikari, and S. Succi, J. Comput. Phys. **234**, 1 (2013); e-print arXiv:1202.3299.
[60]R. Rubinstein and L.-S. Lo, Phys. Rev. E **77**, 036709 (2008).
[61]F. S. Bates and G. H. Fredrickson, Phys. Today **52**, 32 (1999).
[62]I. W. Hamley, *The Physics of Block Copolymers* (Oxford University Press, U.K., 1998).
[63]S. W. Sides, B. J. Kim, E. J. Kramer, and G. H. Fredrickson, Phys. Rev. Lett. **96**, 250601 (2006).
[64]A. W. Bosse, C. J. Garcia-Cervera, and G. H. Fredrickson, Macromolecules **40**, 9570 (2007).
[65]I. Bita, J. K. W. Yang, Y. S. Jung, C. A. Ross, E. L. Thomas, and K. K. Berggren, Science **321**, 939 (2008).
[66]J. Y. Cheng, C. T. Rettner, D. P. Sanders, H. C. Kim, and W. D. Hinsberg, Adv. Mater. **20**, 3155 (2008).
[67]R. Ruiz, H. Kang, F. A. Detcheverry, E. Dobisz, D. S. Kercher, T. R. Albrecht, J. J. De Pablo, and P. F. Nealey, Science **321**, 936 (2008).
[68]S. Park, D. H. Lee, J. Xu, B. Kim, S. W. Hong, U. Jeong, T. Xu, and T. P. Russell, Science **323**, 1030 (2009).
[69]J.-B. Chang, J. G. Son, A. F. Hannon, A. Alexander-Katz, C. A. Ross, and K. K. Berggren, ACS Nano **6**, 2071 (2012).
[70]K. T. Delaney and G. H. Fredrickson, e-print arXiv:1204.5434.
[71]J. Toelke and M. Krafczyk, Int. J. Comput. Fluid Dyn. **22**, 443 (2008).
[72]A. Kaufman, Z. Fan, and K. Petkov, J. Stat. Mech.: Theory Exp. (**2009**) P06016.
[73]F. Nannelli and S. Succi, J. Stat. Phys. **68**, 401 (1992).
[74]I. V. Karlin, S. Succi, and S. Orszag, Phys. Rev. Lett. **82**, 5245 (1999).
[75]N. Rossi, S. Ubertini, G. Bella, and S. Succi, Int. J. Numer. Methods Fluids **49**, 619 (2005).
[76]Z.-G. Feng and E. E. Michaelides, J. Comput. Phys. **195**, 602 (2004).